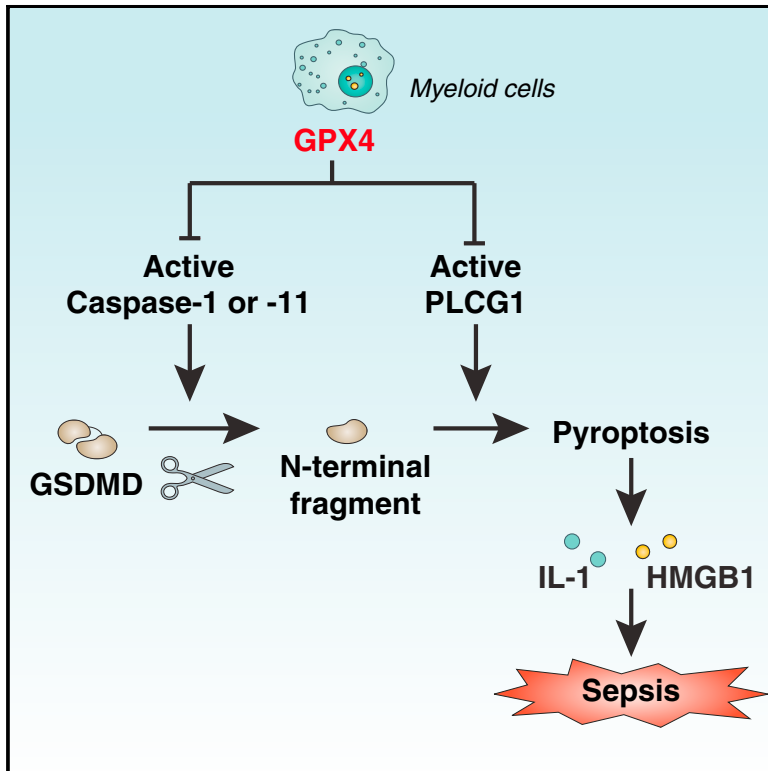


Cell Host & Microbe

Lipid Peroxidation Drives Gasdermin D-Mediated Pyroptosis in Lethal Polymicrobial Sepsis

Graphical Abstract



Authors

Rui Kang, Ling Zeng, Shan Zhu, ..., Timothy R. Billiar, Jianxin Jiang, Daolin Tang

Correspondence

jiangjx@cta.cq.cn (J.J.), tangd2@upmc.edu (D.T.)

In Brief

Kang et al. demonstrate that glutathione peroxidase 4 (GPX4) serves a protective role in mice undergoing septic shock. Myeloid-specific deficiency of *Gpx4* coordinates lipid peroxidation-dependent caspase-11 activation and gasdermin D-mediated pyroptosis during polymicrobial sepsis. Vitamin E administration reverses *Gpx4*^{Mye-/-} susceptibility, thereby revealing a potential target for therapeutic intervention for lethal infection.

Highlights

- *Gpx4* deficiency in myeloid cells increases severity of polymicrobial sepsis in mice
- Caspase-11-dependent pyroptosis mediates septic death in *Gpx4*^{Mye-/-} mice
- GPX4 decreases lipid peroxidation to block PLCG1-mediated GSDMD activity and pyroptosis
- Antioxidant activity of vitamin E promotes survival during sepsis in *Gpx4*^{Mye-/-} mice

Lipid Peroxidation Drives Gasdermin D-Mediated Pyroptosis in Lethal Polymicrobial Sepsis

Rui Kang,^{1,2} Ling Zeng,³ Shan Zhu,¹ Yangchun Xie,⁴ Jiao Liu,¹ Qirong Wen,¹ Lizhi Cao,⁵ Min Xie,⁵ Qitao Ran,⁶ Guido Kroemer,^{7,8,9,10,11,12,13} Haichao Wang,¹⁴ Timothy R. Billiar,² Jianxin Jiang,^{3,*} and Daolin Tang^{1,2,15,*}

¹The Third Affiliated Hospital, Center for DAMP Biology, Key Laboratory for Major Obstetric Diseases of Guangdong Province, Key Laboratory of Protein Modification and Degradation Laboratory of Guangdong Higher Education Institutes, School of Basic Medical Sciences, Guangzhou Medical University, Guangzhou, Guangdong 510510, China

²Department of Surgery, University of Pittsburgh, Pittsburgh, PA 15219, USA

³State Key Laboratory of Trauma, Burns and Combined Injury, Research Institute of Surgery, Research Institute for Traffic Medicine of People's Liberation Army, Daping Hospital, Third Military Medical University, Chongqing 400042, China

⁴Department of Oncology, The Second Xiangya Hospital of Central South University, Changsha, Hunan 410008, China

⁵Department of Pediatrics, Xiangya Hospital, Central South University, Changsha, Hunan 410008, China

⁶Department of Cell Systems and Anatomy, University of Texas Health Science Center, Research Service, South Texas Veterans Health Care System, San Antonio, TX 78229, USA

⁷Université Paris Descartes, Sorbonne Paris Cité, 75006 Paris, France

⁸Equipe 11 Labellisée Ligue Nationale Contre le Cancer, Centre de Recherche des Cordeliers, 75006 Paris, France

⁹Institut National de La Santé et de La Recherche Médicale, U1138 Paris, France

¹⁰Université Pierre et Marie Curie, 75006 Paris, France

¹¹Metabolomics and Cell Biology Platforms, Gustave Roussy Cancer Campus, 94800 Villejuif, France

¹²Pôle de Biologie, Hôpital Européen Georges Pompidou, AP-HP, 75015 Paris, France

¹³Department of Women's and Children's Health, Karolinska University Hospital, 17176 Stockholm, Sweden

¹⁴Laboratory of Emergency Medicine, North Shore University Hospital, The Feinstein Institute for Medical Research, Manhasset, NY 11030, USA

¹⁵Lead Contact

*Correspondence: jiangjx@cta.cq.cn (J.J.), tangd2@upmc.edu (D.T.)

<https://doi.org/10.1016/j.chom.2018.05.009>

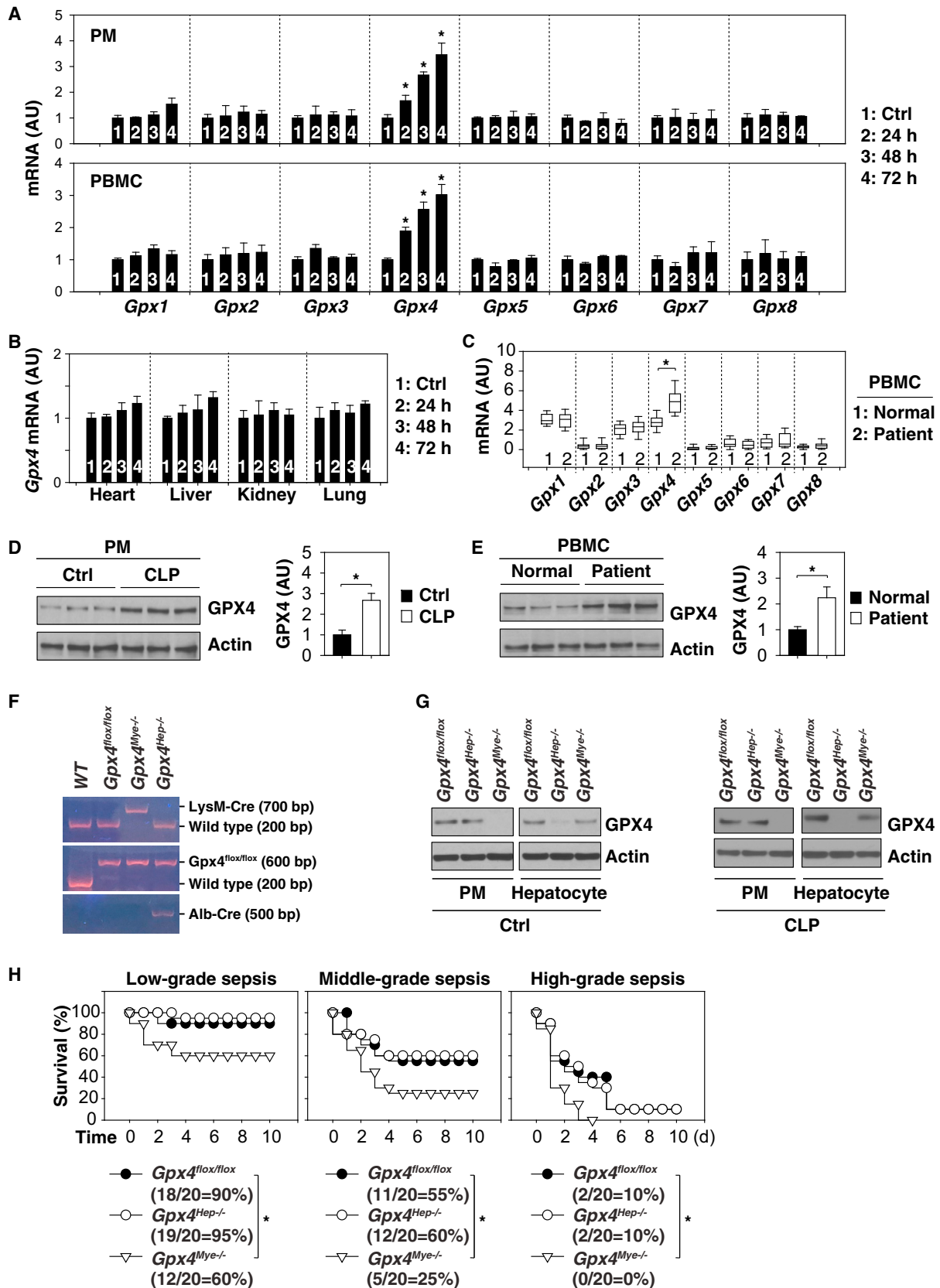
SUMMARY

Sepsis is a life-threatening condition caused by pathogen infection and associated with pyroptosis. Pyroptosis occurs upon activation of proinflammatory caspases and their subsequent cleavage of gasdermin D (GSDMD), resulting in GSDMD N-terminal fragments that form membrane pores to induce cell lysis. Here, we show that antioxidant defense enzyme glutathione peroxidase 4 (GPX4) and its ability to decrease lipid peroxidation, negatively regulate macrophage pyroptosis, and septic lethality in mice. Conditional *Gpx4* knockout in myeloid lineage cells increases lipid peroxidation-dependent caspase-11 activation and GSDMD cleavage. The resultant N-terminal GSDMD fragments then trigger macrophage pyroptotic cell death in a phospholipase C gamma 1 (PLCG1)-dependent fashion. Administration of the antioxidant vitamin E that reduces lipid peroxidation, chemical inhibition of PLCG1, or genetic *Caspase-11* deletion or *Gsdmd* inactivation prevents polymicrobial sepsis in *Gpx4*^{-/-} mice. Collectively, this study suggests that lipid peroxidation drives GSDMD-mediated pyroptosis and hence constitutes a potential therapeutic target for lethal infection.

INTRODUCTION

Sepsis and septic shock are frequently lethal complications of bacterial infections, accounting for approximately 250,000 deaths per year in the US alone (Singer et al., 2016). Although infection-elicited inflammatory responses are crucial for host defense against invading microbes (Jorgensen et al., 2017), excessive activation of innate immune cells such as macrophages may contribute to tissue damage and multiple organ failure. Pyroptosis, an inflammatory form of regulated necrosis, occurs as a consequence of the activation of caspase-1 and caspase-11 in macrophages (Man and Kanneganti, 2016). It has recently been shown that the cleavage of gasdermin D (GSDMD) by caspase-1 and caspase-11 constitutes a critical event in the lethal cascade leading to infection-associated pyroptotic cell death (Kayagaki et al., 2015; Shi et al., 2015). Indeed, the N-terminal fragment of GSDMD (GSDMD-N) can bind to inner membrane lipids, forming pores in the plasma membrane that ultimately result in cellular lysis (Kayagaki et al., 2015; Shi et al., 2015).

Cytoplasmic membrane lipid peroxidation, an auto-oxidative process initiated by the attack of free radicals, contributes to the progression of various types of regulated cell death (Gaschler and Stockwell, 2017). However, it remains unknown whether lipid peroxidation contributes to GSDMD-mediated pyroptosis during lethal infection. Here, we demonstrate that glutathione peroxidase 4 (GPX4), an antioxidant defense enzyme active in repairing oxidative damage to lipids, is an important negative regulator of macrophage pyroptosis. Genetic inactivation of



(legend on next page)

GPX4 increases lipid peroxidation, thus exacerbating GSDMD-mediated pyroptosis in macrophages as well as septic lethality in mice. Thus, our findings uncover a critical mechanism that controls lipid peroxidation in the context of infection-induced lethality.

RESULTS

Gpx4 Deficiency in Myeloid Cells Results in Increased Susceptibility to Polymicrobial Infection

Mammalian glutathione peroxidases (GPXs) including GPX1-8 are functional antioxidant defense enzymes that protect cells from oxidative damage (Brigelius-Flohe and Maorino, 2013). To understand the roles of GPXs in polymicrobial infections, we quantified the expression of *Gpx1-8* in peritoneal macrophages (PMs) and peripheral blood mononuclear cells (PBMCs) from C57BL/6 mice subjected to cecal ligation and puncture (CLP), a well-established animal model of polymicrobial infection. Unlike most other *Gpx* family members, *Gpx4* mRNA was time-dependently upregulated in PMs and PBMCs from septic mice (Figure 1A). In contrast, experimental sepsis failed to significantly alter *Gpx4* mRNA levels in the heart, liver, kidney, and lung (Figure 1B). Of note, the mRNA levels of *Gpx4* (but not *Gpx1*, *Gpx2*, *Gpx3*, *Gpx5*, *Gpx6*, *Gpx7*, and *Gpx8*) were also upregulated in PBMCs from septic patients compared with the healthy control group (Figure 1C). Consistently, GPX4 protein expression was similarly increased in mouse PMs (Figure 1D) and human PBMCs (Figure 1E) under septic conditions. These findings indicate that *Gpx4* is specifically upregulated in innate immune cells during the course of experimental and clinical sepsis.

To define the role of GPX4 in polymicrobial infection, we generated myeloid cell-specific (*LysM-Cre;Gpx4^{fllox/fllox}*, termed *Gpx4^{Mye-/-}* mice) and hepatocyte-specific *Gpx4*-knockout mice (*Alb-Cre;Gpx4^{fllox/fllox}*, termed *Gpx4^{Hep-/-}* mice) (Figure 1F). Immunoblot analysis confirmed a diminished GPX4 protein expression in PMs and hepatocytes from *Gpx4^{Mye-/-}* and *Gpx4^{Hep-/-}* mice, respectively (Figure 1G). Remarkably, *Gpx4^{Mye-/-}* mice, but not *Gpx4^{Hep-/-}* mice, were significantly more susceptible to death induced by low-, middle-, and high-grade polymicrobial sepsis than control *Gpx4^{fllox/fllox}* mice (Figure 1H). Thus, *Gpx4* expressed in the myeloid lineage cells, but not in hepatocytes, functions as an endogenous inhibitor of lethal sepsis.

Vitamin E and Caspase Inhibitor Protect against Sepsis in Mice

To define the molecular mechanisms underlying GPX4-mediated protection against polymicrobial infection, we treated mice with the antioxidant vitamin E and examined the contribution of oxidative injury to septic shock. Although vitamin E protected against CLP-induced animal lethality in both *Gpx4^{fllox/fllox}* and *Gpx4^{Mye-/-}* mice, vitamin E exhibited a greater increase in animal survival for *Gpx4^{Mye-/-}* mice than *Gpx4^{fllox/fllox}* mice (50% versus 30%, Figure 2A). The serum levels of lipid peroxidation products (e.g., malondialdehyde [MDA] and 4-hydroxynonenal [4-HNE]) and markers indicating organ dysfunction (e.g., creatine kinase [CK], blood urea nitrogen [BUN], and alanine aminotransferase [ALT]) were all increased in septic *Gpx4^{Mye-/-}* mice compared with septic *Gpx4^{fllox/fllox}* mice (Figure 2B). Vitamin E administration significantly attenuated the sepsis-induced elevation of serum MDA, 4-HNE, CK, BUN, and ALT levels (Figure 2B), supporting the notion that oxidative injury contributes to septic lethality. As expected, there were no significant phenotype differences between *Gpx4^{fllox/fllox}* and *Gpx4^{Mye-/-}* mice after sham surgery (Figures 2A and 2B).

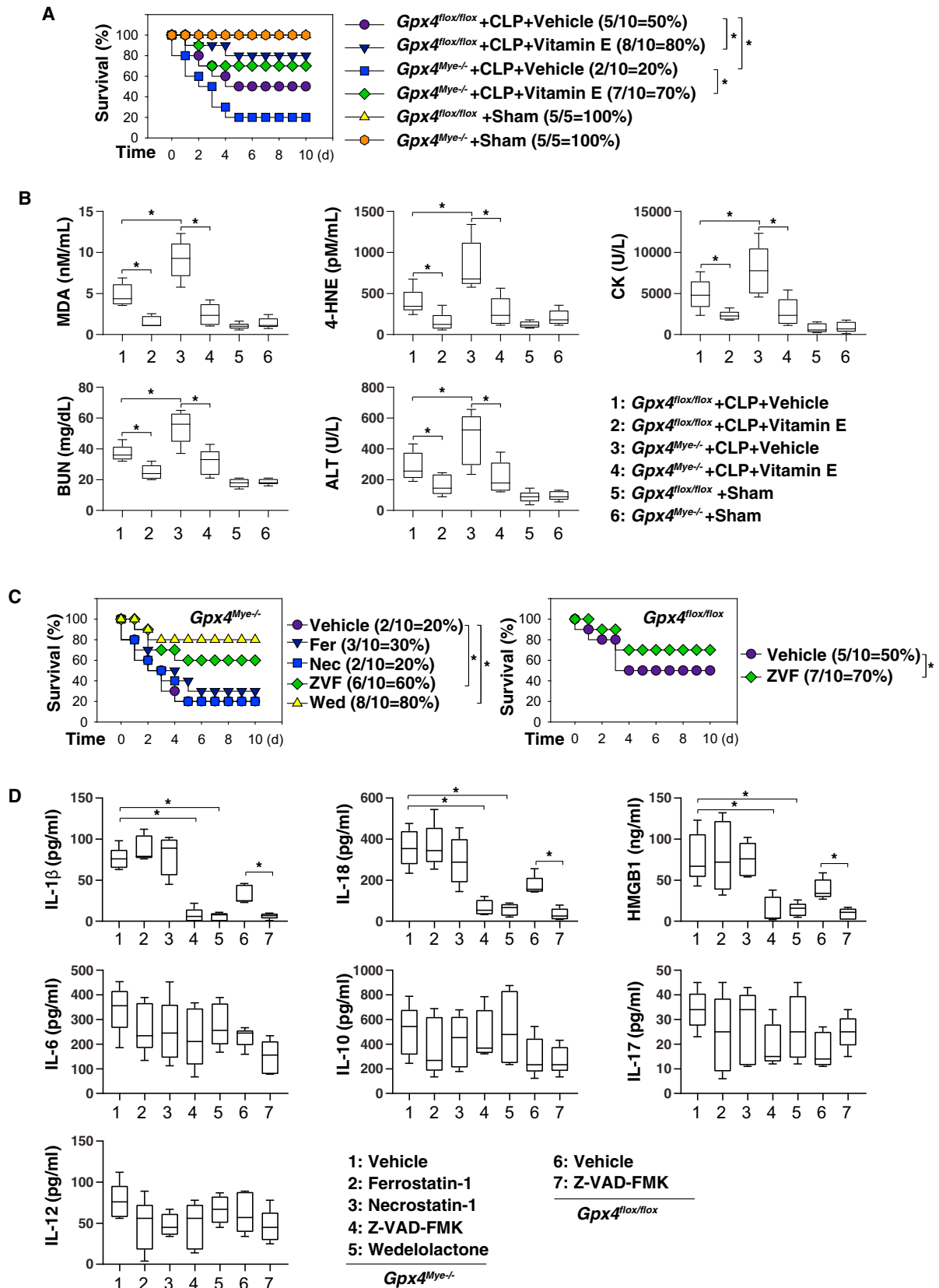
Gpx4 deficiency-induced lipid peroxidation has been implicated in the progression of regulated cell death, including apoptosis (Ran et al., 2003; Seiler et al., 2008), necroptosis (Canli et al., 2016), and ferroptosis (Friedmann Angeli et al., 2014; Yang et al., 2014b). Importantly, administration of a specific inhibitor for ferroptosis (ferrostatin-1) or necroptosis (necrostatin-1) failed to affect CLP-induced septic lethality in *Gpx4^{Mye-/-}* mice (Figure 2C). In contrast, administration of Z-VAD-FMK (a pan caspase inhibitor) or wedelolactone (an inhibitor of caspase-11) to *Gpx4^{Mye-/-}* mice conferred significant protection against lethal sepsis (Figure 2C). Similarly, Z-VAD-FMK also partly protected against CLP-induced septic death in *Gpx4^{fllox/fllox}* mice (Figure 2C). Furthermore, the sepsis-induced elevation of serum levels of inflammatory-dependent cytokines (e.g., interleukin-1 β [IL-1 β], IL-18, and HMGB1), but not inflammasome-independent cytokines (e.g., IL-6, IL-10, IL-17, and IL-12), was attenuated by the administration of Z-VAD-FMK or wedelolactone, but not by ferrostatin-1 or necrostatin-1 (Figure 2D). Collectively, these findings suggest a major role for pyroptosis in the pathogenesis of lethal sepsis.

Caspase-11-Dependent Pyroptosis Mediates Septic Death in *Gpx4^{Mye-/-}* Mice

It has been shown that global knockout of *caspase-11* has no impact on CLP-induced sepsis (Vanden Berghie et al., 2014)

Figure 1. *Gpx4* Deficiency in Myeloid Cells Results in Increased Susceptibility to Polymicrobial Infection

- (A) qPCR analysis of *Gpx1-8* mRNA in PMs or PBMCs from septic mice at 24–72 hr (n = 3 mice/group; data are expressed as means \pm SD, *p < 0.05 versus control group, t test).
- (B) qPCR analysis of *Gpx1-8* mRNA in the indicated tissues from septic mice at 24–72 hr (n = 3 mice/group; data are expressed as means \pm SD).
- (C) Boxplots comparing *Gpx1-8* mRNA levels in PBMC samples from septic patients (n = 16) and healthy controls (n = 16). The mRNAs are presented as median value (black line), interquartile range (box), and minimum and maximum of all data (black line). *p < 0.05 versus control group, t test.
- (D) Western blot analysis of GPX4 protein expression in mouse PMs from control group or septic mice at 72 hr (n = 3 mice/group; data expressed as means \pm SD, *p < 0.05, t test).
- (E) Western blot analysis of GPX4 protein expression in human PBMCs or septic patients at hospital admission (n = 3 patient/group; data expressed as means \pm SD, *p < 0.05, t test).
- (F) Genotype identification of transgenic mice based on reverse transcription PCR.
- (G) Western blot analysis of GPX4 expression in PMs and hepatocytes from *Gpx4^{fllox/fllox}*, *Gpx4^{Hep-/-}*, or *Gpx4^{Mye-/-}* mice with or without CLP for 72 hr.
- (H) Mice with the indicated genotypes were subjected to CLP with syringe needles with gauges ranging from 27 (A) (“low-grade sepsis”), 22 (B) (“middle-grade sepsis”), to 17 (C) (“high-grade sepsis”). Animal survival was assayed (n = 20 mice/group; *p < 0.05, Kaplan-Meier survival analysis).



but protects against lethal endotoxemia (Hagar et al., 2013). Moreover, conditional knockout of *caspase-11* in endothelial cells confers similar protection against lipopolysaccharide (LPS)- and CLP-induced acute lung injury and lethality in mice (Cheng et al., 2017), suggesting a cell-type-dependent role of caspase-11 in sepsis.

To test whether caspase-11-dependent pyroptosis is required for lethal inflammation in septic *Gpx4*^{Mye-/-} mice, we generated *Caspase-11* and *Gpx4* double knockout mice using myeloid lineage cells (*LysM-Cre;Gpx4*^{flox/flox};*Casp11*^{flox/flox}, termed *Gpx4*^{Mye-/-}*Casp11*^{Mye-/-} mice). Compared with *Gpx4*^{flox/flox} controls, *Casp11*^{Mye-/-} or *Gpx4*^{Mye-/-}*Casp11*^{Mye-/-} mice exhibited increased survival (Figure 3A), with decreased serum levels of IL-1 β , IL-18, HMGB1, CK, BUN, and ALT, but not IL-6 and IL-10, during experimental sepsis (Figure 3B), supporting an essential role for caspase-11 in mediating lethal inflammation and tissue injury.

Although pyroptotic macrophages may have the ability to clear bacteria (Jorgensen et al., 2016), the number of bacterial colony-forming units recovered from the blood and peritoneal lavage after CLP did not significantly differ between *Gpx4*^{Mye-/-} and *Gpx4*^{Mye-/-}*Casp11*^{Mye-/-} mice (Figure 3C). In light of the tremendous impact of altered microbiota on the outcome of CLP sepsis (Wilmore et al., 2018), it will be interesting to examine whether *Gpx4* deficiency causes microbiome variation in independent studies.

GPX4 Blocks GSDMD Cleavage During Inflammasome Activation

The cleavage and formation of activated N-terminal domain of GSDMD (GSDMD-N) by inflammatory caspases is a recently identified executioner of pyroptosis (Aglietti et al., 2016; Ding et al., 2016; Liu et al., 2016; Sborgi et al., 2016). We next investigated whether, in lieu of suppressing bacterial elimination, GPX4 regulated the cleavage of GSDMD following inflammasome activation. Caspase-11-mediated non-canonical inflammasome activation requires at least two signals (Kayagaki et al., 2015; Shi et al., 2015). The first signal (signal 1), also known as the priming signal, is triggered by microbial products or proinflammatory cytokines, such as interferon- γ (IFN- γ), which are recognized by macrophage pattern recognition and cytokine receptors (Kayagaki et al., 2015; Rathinam et al., 2012). Signal 1 activates the nuclear factor κ B pathway, leading to upregulation of pro-IL-1 β and pro-caspase-11 protein levels (Kayagaki et al., 2015). However, the loss of *Gpx4* failed to affect Toll-like receptor ligands (e.g., LPS, poly(I:C), and Pam3CSK4), and IFN- γ -induced pro-IL-1 β and pro-caspase-11 protein (Figure 4A) and mRNA (Figure 4B) expression in bone marrow-derived mac-

rophages (BMDMs). The second signal (signal 2) is mediated by cytosolic LPS or bacterial infection, resulting in caspase-11-dependent GSDMD cleavage to generate activated GSDMD-N (Kayagaki et al., 2015; Shi et al., 2015). We observed that the loss of *Gpx4* increased GSDMD-N formation, proteolytic IL-1 β maturation (p17), and caspase-11 (p26) activation in BMDMs following LPS electroporation or *Escherichia coli* infection (Figure 4C). This process was blocked by caspase-11 depletion (Figure 4C). Consistently, the LPS electroporation- or *E. coli* infection-induced cytotoxicity and associated extracellular release of lactate dehydrogenase, IL-1 β , and HMGB1 was increased in *Gpx4*^{-/-}, but not in *Casp11*^{-/-} or *Gpx4*^{-/-}*Casp11*^{-/-} BMDMs (Figure 4D).

In addition to the non-canonical (caspase-11-dependent) inflammasome, the canonical (caspase-1-dependent) NLRP3 inflammasome contributes to GSDMD cleavage under certain conditions (He et al., 2015; Kayagaki et al., 2015; Shi et al., 2015). Indeed, a classical NLRP3 inflammasome activator induced GSDMD-N formation (Figure 4E), caspase-1 (p20) activation (Figure 4E), cytotoxicity (Figure 4F), and consequent release of matured IL-1 β (p17) (Figure 4F) and HMGB1 (Figure 4F) in LPS-primed *Gpx4*^{-/-}, *Casp11*^{-/-}, or *Gpx4*^{-/-}*Casp11*^{-/-}, but not in *Nlrp3*^{-/-}, *Casp1*^{-/-}*Casp11*^{-/-}, *Gpx4*^{-/-}*Nlrp3*^{-/-} or *Gpx4*^{-/-}*Casp1*^{-/-}*Casp11*^{-/-} BMDMs. Consistent with previous studies (Kayagaki et al., 2011; Py et al., 2014), ATP failed to induce caspase-11 activation in macrophages (Figure 4E). Collectively, these findings indicate that GPX4 functions as an endogenous repressor of caspase-11- or caspase-1-mediated cleavage of GSDMD in activated macrophages.

Oxidation of Phospholipids Promotes GSDMD-N-Mediated Pyroptosis

We next investigated the impact of GPX4 on GSDMD-N-induced pyroptosis. Consistent with a previous study (Shi et al., 2015), transfection with GSDMD-N (1–276), but not GSDMD-C (277–487), GSDMD cleavage mutant (D275A), or full-length GSDMD-FL (1–487), induced cytotoxicity to BMDMs (Figure 5A). The GSDMD-N-mediated cytotoxicity was further increased in *Gpx4*^{-/-} BMDMs (Figure 5A), but was reversed by vitamin E supplementation or enforced expression of *Gpx4* (Figure 5A). In contrast, GSDMD-N-induced cytotoxicity was not reversed by the depletion of *Caspase-1* and *Caspase-11* or enforced expression of a catalytically inactive *Gpx4* cDNA (U46S mutant) (Manes et al., 2011) in *Gpx4*^{-/-} BMDMs (Figure 5A), indicating that caspase-1 and caspase-11 are not essential for GSDMD-N-mediated cytotoxicity despite their involvement in the generation of GSDMD-N.

Figure 2. Effects of Vitamin E and Cell Death Inhibitors on Sepsis in Mice

- (A) Analysis of animal survival in mice with or without repeated intraperitoneal administration of vitamin E (500 mg/kg) at 3, 24, 48, and 72 hr after CLP (22-gauge needle)-induced sepsis (n = 5–10 mice/group; *p < 0.05, Kaplan-Meier survival analysis).
- (B) In parallel, serum levels of MDA, 4-HNE, CK, BUN, and ALT were assayed at 72 hr after CLP (n = 5 mice/group; *p < 0.05, ANOVA least significant difference [LSD] test). Data are presented as median value (black line), interquartile range (box), and minimum and maximum of all data (black line).
- (C) Analysis of animal survival in mice with or without repeated intraperitoneal administration of Z-VAD-FMK ("ZVF," 5 mg/kg), wedelolactone ("Wed," 20 mg/kg), ferostatin-1 ("Fer," 10 mg/kg), or necrostatin-1 ("Nec," 5 mg/kg) at 3, 24, 48, and 72 hr after CLP (22-gauge needle)-induced sepsis (n = 10 mice/group; *p < 0.05, Kaplan-Meier survival analysis).
- (D) In parallel, serum levels of IL-1 β , IL-18, HMGB1, IL-6, IL-10, IL-17, and IL-12 were assayed at 72 hr after CLP (n = 5 mice/group; *p < 0.05, ANOVA LSD test). Data are presented as median value (black line), interquartile range (box), and minimum and maximum of all data (black line).

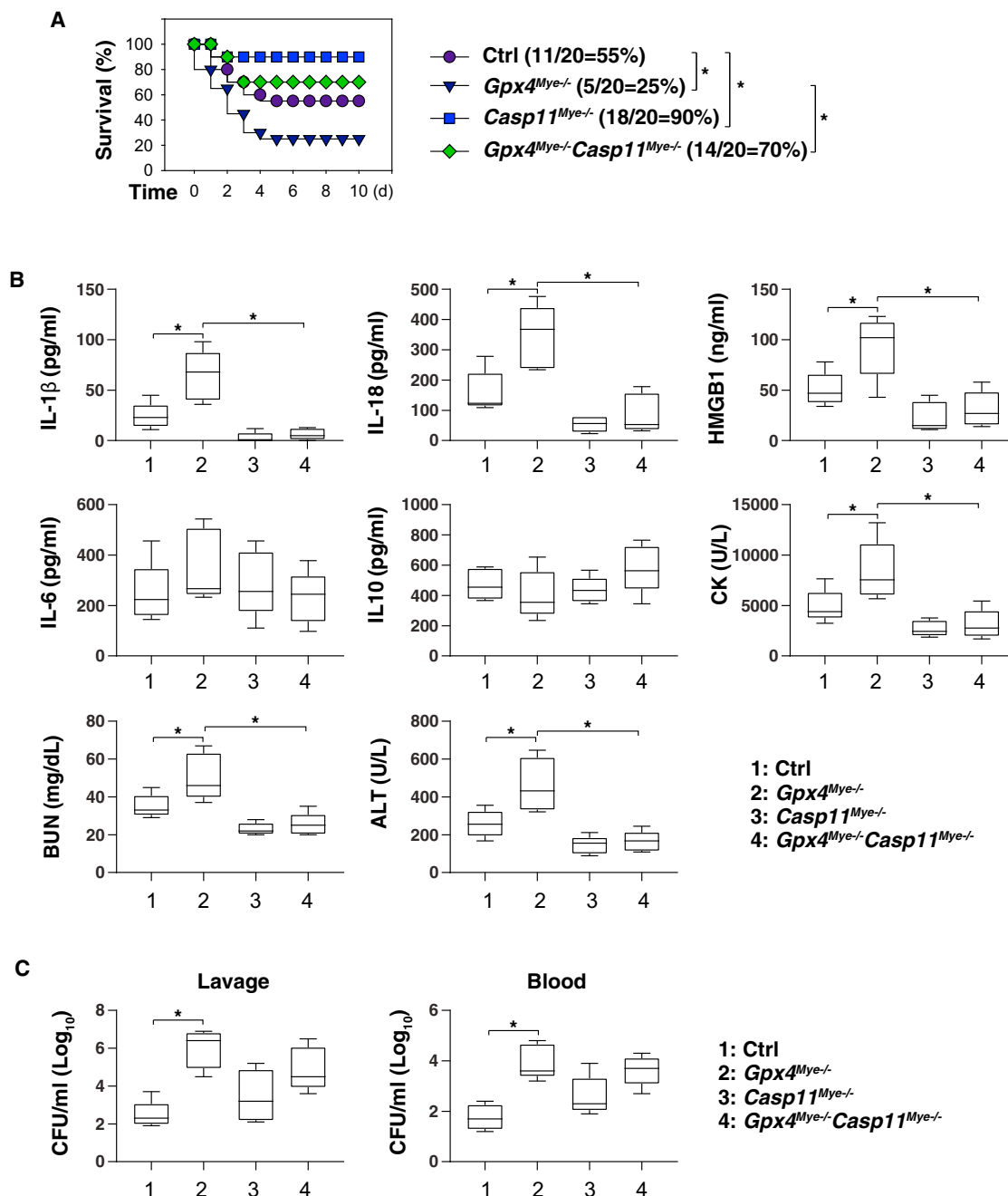


Figure 3. Caspase-11-Dependent Pyroptosis Mediates Septic Death in *Gpx4^{Myc-/-}* Mice

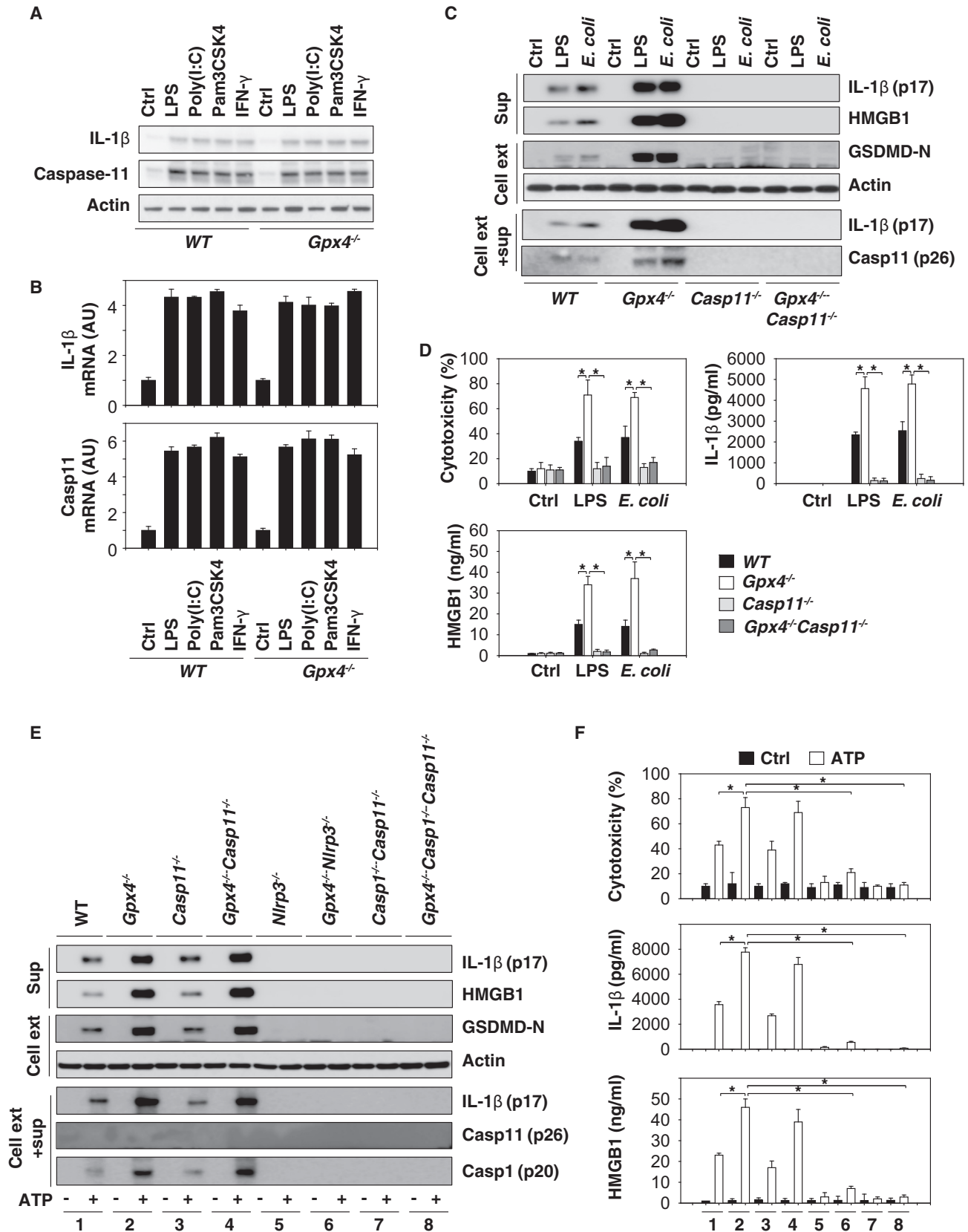
(A) Mice with the indicated genotypes were subjected to CLP with 22-gauge syringe needles (middle-grade sepsis) and animal survival was monitored (n = 20 mice/group; *p < 0.05, Kaplan-Meier survival analysis). *Gpx4^{Myc-/-}* mice data were the same control as Figure 1H (middle-grade sepsis).

(B) Analysis of serum levels of IL-1 β , IL-18, HMGB1, IL-6, IL-10, CK, BUN, and ALT in middle-grade septic mice at 72 hr (n = 5 mice/group; *p < 0.05, ANOVA LSD test). Data are presented as median value (black line), interquartile range (box), and minimum and maximum of all data (black line).

(C) Analysis of bacterial loading in middle-grade septic mice at 72 hr (n = 5 mice/group; *p < 0.05, ANOVA LSD test). Data are presented as median value (black line), interquartile range (box), and minimum and maximum of all data (black line).

The plasma membrane is a complex mixture of multiple lipids including fatty acids, phospholipids, sterols, and sphingolipids (van Meer et al., 2008). Treatment with several types of phospholipids (e.g., phosphatidylinositol 4-phosphate [PI4P], phosphatidylinositol 4,5-bisphosphate [PI(4,5)P₂], diacylglycerol [DAG],

and phosphatidic acid) sensitized BMDMs to GSDMD-N-induced cytotoxicity (Figure 5B), which was associated with increased MDA production (Figure 5C). In contrast, this process was not affected by the administration of linoleic acid (a polyunsaturated fatty acid), ceramide (a sphingolipid), or cholesterol



(legend on next page)

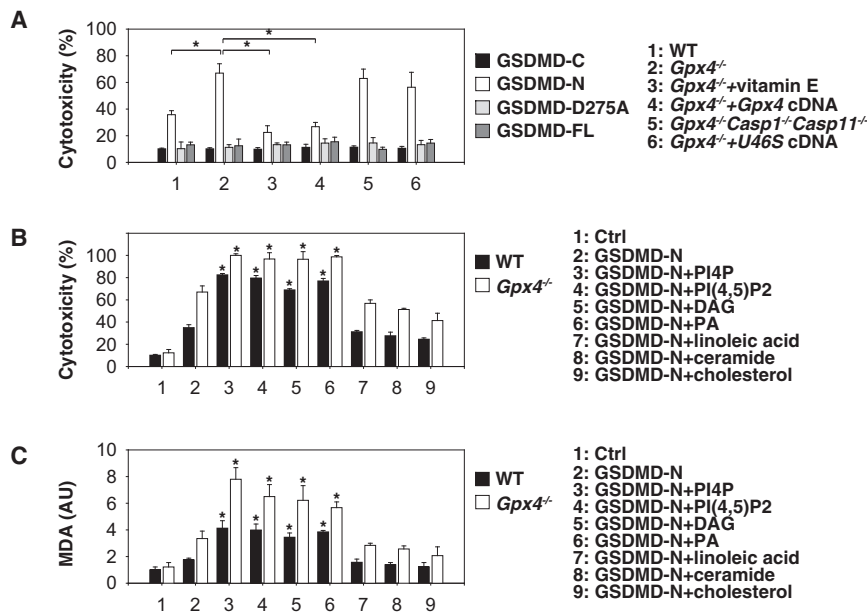


Figure 5. Oxidation of Phospholipids Promote GSDMD-N-Mediated Pyroptosis

(A) WT and *Gpx4*^{-/-} BMDMs were pretreated with vitamin E (100 μM) for 3 hr before transfection with GSDMD-C, GSDMD-N, GSDMD-D275A, or GSDMD-FL expression constructs. Cell viability was assayed within 24 hr of transfection (n = 3 wells/group; means ± SD, *p < 0.05, t test).

(B) WT and *Gpx4*^{-/-} BMDMs were pretreated with the indicated lipid components (20 μM) for 3 hr, and then transfected with GSDMD-N. Cell viability was assayed within 24 hr of transfection (n = 3 wells/group; means ± SD, *p < 0.05 versus GSDMD-N group, t test).

(C) WT and *Gpx4*^{-/-} BMDMs were pretreated with the indicated lipid components (20 μM) for 3 hr and then transfected with GSDMD-N. Intracellular MDA level was assayed within 24 hr of transfection (n = 3 wells/group; means ± SD, *p < 0.05 versus GSDMD-N group, t test).

(a sterol) (Figures 5B and 5C). Together, these findings suggest that lipid peroxides generated by the oxidation of phospholipids promote GSDMD-N-mediated pyroptosis in BMDMs.

PLC Activation Is Required for N-Terminal GSDMD-Mediated Pyroptosis

Phospholipase C (PLC) mediates the hydrolysis of phospholipid phosphatidylinositol 4,5-bisphosphate (PIP₂) into DAG and inositol 1,4,5-trisphosphate (IP₃), which in turn triggers the activation of calcium signal (Kadamur and Ross, 2013). We therefore investigated whether the increased GSDMD-N-mediated cytotoxicity observed in *Gpx4*^{-/-} BMDMs was associated with PLC activation. Indeed, the phosphorylation of PLC gamma 1 (PLCG1), but not that of PLC beta 3 (PLCB3), was increased in *Gpx4*^{-/-} BMDMs in response to GSDMD-N-mediated pyroptosis (Figure 6A). The GSDMD-N-induced PLCG1 phosphorylation in BMDMs was significantly inhibited by vitamin E (Figure 6A), suggesting that oxidative stress induces PLCG1 activation. Notably, shRNA-mediated depletion of *Plcg1* and addition of the pharmacological PLC inhibitor U73122 similarly inhibited GSDMD-N-induced pyroptosis, which was associated with a decreased production of DAG and IP₃, as well as a reduced intracellular calcium influx (Figure 6B). The calcium chelator BAPTA-AM blocked GSDMD-

N-induced pyroptosis and calcium influx, but not DAG and IP₃ production (Figure 6B). These findings indicate that GSDMD-N-mediated activation of calcium signaling is downstream of PLCG1-mediated DAG and IP₃ production (Hayashi et al., 2007; Pocock and Bates, 2001).

Knockdown of PLCG1 also blocked GSDMD-N-mediated cytotoxicity in THP1 (human monocytic leukemia cell line), HL-60 (human promyelocytic leukemia cell line), and HeLa (human cervical cancer) cells (Figure 6C). Moreover, exogenous PI4P, but not linoleic acid, ceramide, or cholesterol, enhanced GSDMD-N-induced PLCG1 phosphorylation (Figure 6D), suggesting a possible reciprocal relationship between PLCG1 activation and PIP₂ metabolism during GSDMD-N-induced pyroptosis. The knockdown of *Plcg1* and administration of U73122 or BAPTA-AM similarly inhibited GSDMD-N-induced cell death in the presence of phospholipids (PI4P and PI(4,5)P2) (Figure 6E), supporting a possible association between Ca²⁺ elevation and lipid peroxidation during GSDMD-N-induced pyroptosis (Aglietti et al., 2016; Liu et al., 2016).

Of note, genetic or pharmacologic inhibition of *Plcg1* by shRNA or using U73122 similarly attenuated the LPS electroporation- or *E. coli* infection-induced cytotoxicity (Figure 6F) without affecting the production of active caspase-11 (p26), GSDMD-N, and matured IL-1β (p17) (Figure 6G). Collectively,

Figure 4. GPX4 Blocks GSDMD Cleavage during Inflammasome Activation

(A) Western blot analysis of IL-1β and caspase-11 protein expression in BMDMs following treatment with LPS (500 ng/mL), poly(I:C) (5 μg/mL), Pam3CSK4 (1 μg/mL), or IFN-γ (10 ng/mL) for 6 hr.

(B) qPCR analysis of IL-1β and caspase-11 mRNA expression in BMDMs following treatment with LPS (500 ng/mL), poly(I:C) (5 μg/mL), Pam3CSK4 (1 μg/mL), or IFN-γ (10 ng/mL) for 6 hr.

(C) Western blot analysis of indicated proteins in BMDMs recovered from mice with the indicated genotypes following LPS electroporation or *E. coli* (MOI = 25) infection for 16 hr. Sup, supernatants.

(D) In parallel, cytotoxicity (lactate dehydrogenase release) and levels of IL-1β and HMGB1 in the supernatant were assayed (n = 3 wells/group; data expressed as means ± SD, *p < 0.05, ANOVA LSD test).

(E) Western blot analysis of LPS (500 ng/mL)-primed indicated BMDMs following treatment with ATP (5 mM) for 1 hr. Sup, supernatants.

(F) In parallel, cytotoxicity and levels of IL-1β and HMGB1 in the supernatant were assayed (n = 3 wells/group; data expressed as means ± SD, *p < 0.05, ANOVA LSD test).

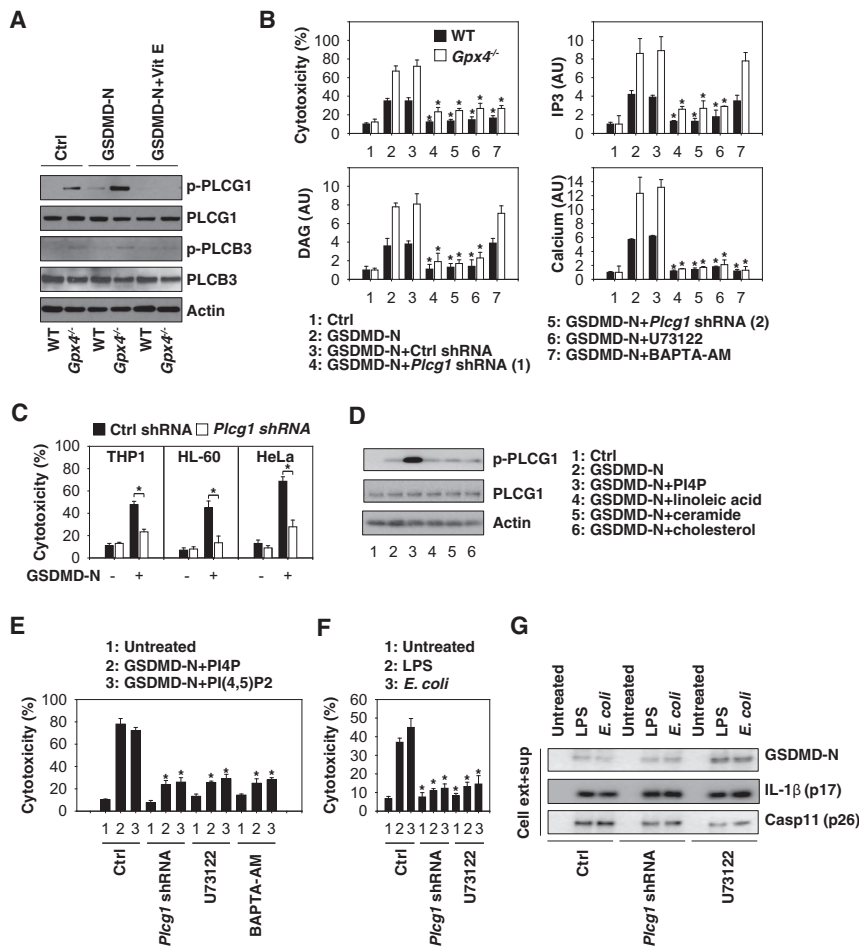


Figure 6. PLC Activation Contributes to GSDMD-Mediated Pyroptosis

(A) WT and *Gpx4*^{-/-} BMDMs were pretreated with or without vitamin E (100 μ M) for 3 hr, and then transfected with GSDMD-N. Protein expression was assayed using western blot.

(B) Analysis of GSDMD-N-mediated cytotoxicity, DAG, IP₃, and calcium production at 24 hr in WT and *Gpx4*^{-/-} BMDMs in the absence or presence of *Plcg1*-shRNA, U73122 (10 μ M), or BAPTA-AM (10 μ M) (n = 3 wells/group; data expressed as means \pm SD, *p < 0.05 versus GSDMD-N group, t test).

(C) Analysis of GSDMD-N-mediated cytotoxicity at 24 hr in THP1, HL-60, and HeLa cell lines (n = 3 wells/group; data expressed as means \pm SD, *p < 0.05, t test).

(D) WT BMDMs were pretreated with the indicated lipid components (20 μ M) for 3 hr, and then transfected with GSDMD-N for 24 hr. Protein expression was assayed using western blot.

(E) Analysis of GSDMD-N/PI4P- or GSDMD-N/PI(4,5)P₂-mediated cytotoxicity at 24 hr in BMDMs in the absence or presence of *Plcg1*-shRNA, U73122 (10 μ M), or BAPTA-AM (10 μ M) (n = 3 wells/group; data expressed as means \pm SD, *p < 0.05 versus control group, t test).

(F) Analysis of LPS electroporation- or *E. coli* (MOI = 25) infection-mediated cytotoxicity at 16 hr in BMDMs in the absence or presence of *Plcg1*-shRNA or U73122 (10 μ M) (n = 3 wells/group; data expressed as means \pm SD, *p < 0.05 versus control group, t test).

(G) Analysis of LPS electroporation- or *E. coli* (MOI = 25) infection-mediated protein expression at 16 hr in BMDMs in the absence or presence of *Plcg1*-shRNA or U73122 (10 μ M).

these findings suggest that phospholipid peroxidation-mediated PLCG1 activation may contribute to GSDMD-N-mediated cytotoxicity without affecting GSDMD-N production.

PLC Activation Is Required for N-Terminal GSDMD-Mediated Septic Death

To determine whether GSDMD activation contributes to septic death of *Gpx4*^{Mye-/-} mice, we used backcrossed *Gsdmd*^{I105N/I105N} mice (which bear a GSDMD cleavage site mutation that renders the protein resistant to proteolytic activation by caspase-1 or -11) in the *Gpx4*^{Mye-/-} background to generate *LysM-Cre;Gpx4*^{fllox/fllox;Gsdmd}^{I105N/I105N} (in short *Gpx4*^{Mye-/-} *Gsdmd*^{-/-}) mice. Such GSDMD cleavage mutant mice lacking *Gpx4* in their myeloid cells were protected against CLP-induced lethal sepsis (Figure 7A) with decreased serum levels of CK, BUN, and ALT (Figure 7B) compared with *Gpx4*^{Mye-/-} mice expressing activatable wild-type (WT) GSDMD. Compared with WT control mice, the PLC inhibitor U73122 exhibited greater protection against CLP-induced organ damage and animal lethality in *Gpx4*^{Mye-/-} mice compared with control WT animals (Figures 7A and 7B). Collectively, these animal studies indicate that the caspase-11-GSDMD-PLC pathway contributes to multi-organ failure in septic mice, especially in *Gpx4*^{Mye-/-} mice.

DISCUSSION

Oxidative stress occupies a critical role in the regulation of various biological processes including cell death and innate immunity (Reuter et al., 2010; Ryter et al., 2007). Here, we demonstrate a potential involvement of GPX4 in coordinating lipid peroxidation, inflammasome activation, and pyroptosis during polymicrobial infection. In response to infectious insults, GPX4 is upregulated in innate immune cells to counter-regulate GSDMD-N-mediated pyroptotic cell death, thereby preventing lethal systemic inflammation. These findings therefore establish GPX4 as an essential negative regulator of pyroptosis in lethal inflammation.

In conjunction with antioxidants (e.g., vitamin E), GPX4 catalyzes the reduction of phospholipid hydroperoxides within membranes and lipoproteins to inhibit lipid peroxidation, thereby exerting protection against oxidative stress (Imai and Nakagawa, 2003). Global knockout of *Gpx4* results in early embryonic lethality, while conditional knockout of *Gpx4* in specific organs (e.g., myeloid cells) is compatible with survival into adulthood. Conditional knockout models revealed that *Gpx4* protects against experimental renal failure (Friedmann Angeli et al., 2014), neurodegenerative diseases (Chen et al., 2015), viral and parasitic infections (Matsushita et al., 2015), male

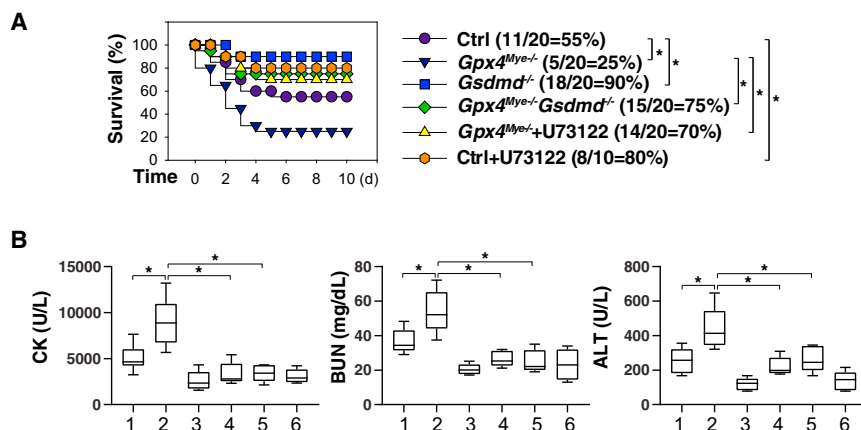


Figure 7. PLC Activation Contributes to GSDMD-Mediated Septic Death

(A) Analysis of animal survival in mice with or without repeated intraperitoneal administration of U73122 (30 mg/kg) at 3, 24, 48, and 72 hr after CLP (22-gauge needle)-induced sepsis (n = 10–20 mice/group; *p < 0.05, Kaplan-Meier survival analysis). *Gpx4*^{Mye-/-} mice data were the same control as Figure 1H (middle-grade sepsis).

(B) In parallel, quantitation of serum CK, BUN, and ALT in middle-grade septic mice at 72 hr (n = 5–8 mice/group; *p < 0.05, ANOVA LSD test). Data are presented as median value (black line), interquartile range (box), and minimum and maximum of all data (black line).

subfertility (Brutsch et al., 2016), atherogenesis (Guo et al., 2008), anemia (Canli et al., 2016), and thrombus formation (Wortmann et al., 2013). *Gpx4* depletion resulted in a marked elevation of apoptosis (Ran et al., 2003; Seiler et al., 2008), necroptosis (Canli et al., 2016), and ferroptosis (Friedmann Angeli et al., 2014; Yang et al., 2014b). The results from the present study indicate that GPX4 also plays a major role in reducing excessive macrophage pyroptosis in the context of sepsis.

We propose that GPX4 serves as a negative regulator of GSDMD cleavage and activation. The generation of GSDMD-N enables its oligomerization to form membrane-damaging pores and to initiate the lethal phase of pyroptosis. The production of GSDMD-N is catalyzed by inflammatory caspases such as caspase-1 and -11 (Aglietti et al., 2016; Ding et al., 2016; He et al., 2015; Kayagaki et al., 2015; Liu et al., 2016; Sborgi et al., 2016; Shi et al., 2015). In contrast to caspase-1-dependent pyroptosis, caspase-11-mediated pyroptosis is triggered by the intracellular invasion of bacteria (Aachoui et al., 2013; Hagar et al., 2013; Kayagaki et al., 2011, 2013). Live *E. coli* and cytosolic LPS require caspase-11, but not caspase-1, to trigger pyroptosis in macrophages (Kayagaki et al., 2011). Specifically, caspase-11 recognizes cytosolic LPS via binding to the lipid A moiety, which results in caspase-11 oligomerization and GSDMD cleavage (Shi et al., 2014). In the present study, we demonstrated that myeloid lineage cell-specific *Gpx4* depletion caused a marked increase in caspase-11- and caspase-1-mediated GSDMD cleavage, suggesting that lipid peroxidation may serve as an accelerator of inflammasome activation and pyroptosis.

It is well-known that GSDMD-N induces pyroptosis only when delivered to the cytosol by transfection, but not when directly added extracellularly, supporting the notion that GSDMD is an endogenous pore-forming protein that inserts itself into the inner leaflet of the plasma membrane (Ding et al., 2016; Liu et al., 2016). The formation of membrane GSDMD pores disrupts the distribution of phospholipids, causing cell swelling (oncosis) and eventual lysis (Aglietti et al., 2016; Ding et al., 2016; Liu et al., 2016; Sborgi et al., 2016). While ferroptosis involves the oxidation of polyunsaturated fatty acids within cell membranes (Kagan et al., 2017; Yuan et al., 2016), our study indicates that oxidation of phospholipids may be involved in GSDMD-N-induced pyroptosis.

Specifically, our data suggest that lipid peroxidation specifically induced the activation of PLCG1 in myeloid cells and that PLCG1 contributes to GSDMD-N-mediated cytotoxicity in a calcium-dependent manner. PLCG1 is a phosphatidylinositol-specific PLC, a class of membrane-associated enzymes that cleaves PIP₂ into DAG and IP₃, resulting in the mobilization of intracellular calcium stores that may contribute to cell death and inflammatory reactions (Kadamur and Ross, 2013). Importantly, the PLC inhibitor U73122 and the calcium chelator BAPTA-AM protect against GSDMD-N cytotoxicity in macrophages or against lethal infection in mice.

In summary, we demonstrated that *Gpx4* expressed by cells from the myeloid lineage plays a major role in attenuating lipid peroxidation, inflammasome activation, and pyroptotic cell death in the context of sepsis. The depletion of *Gpx4* results in increased septic lethality, which is at least partly mediated through caspase-11-mediated GSDMD cleavage and PLCG1-dependent GSDMD-N activation in macrophages. Genetic or pharmacologic inhibition of this pathway reversed the lethal consequences of excessive pyroptosis in the context of sepsis.

STAR★METHODS

Detailed methods are provided in the online version of this paper and include the following:

- KEY RESOURCES TABLE
- CONTACT FOR REAGENT AND RESOURCE SHARING
- EXPERIMENTAL MODEL AND SUBJECT DETAILS
 - Cell Culture
 - Bacterial Infection
 - Animal Model of Sepsis
 - Patient Samples
- METHOD DETAILS
 - Biochemical Assay
 - Calcium Measurement
 - LPS Transfection
 - RNAi and Gene Transfection
 - Western Blot Analysis
 - Quantitative Real-Time Polymerase Chain Reaction
- QUANTIFICATION AND STATISTICAL ANALYSIS
 - Statistical Analysis

SUPPLEMENTAL INFORMATION

Supplemental Information includes two tables and can be found with this article online at <https://doi.org/10.1016/j.chom.2018.05.009>.

ACKNOWLEDGMENTS

We thank Christine Heiner (Department of Surgery, University of Pittsburgh) for her critical reading of the manuscript. This work was supported by grants from the US NIH (R01GM115366, R01CA160417, R01AT005076, R01GM063075, R01GM044100, and R01GM050441), the National Science Foundation of Guangdong Province (2016A030308011), the American Cancer Society (Research Scholar Grant RSG-16-014-01-CDD), the National Natural Science Foundation of China (31671435, 81400132, and 81772508), Guangdong Province Universities and Colleges Pearl River Scholar Funded Scheme (2017), Lin He's Academician Workstation of New Medicine and Clinical Translation (2017), and the International Scientific and Technology Cooperation Program of China (2015DFA31490). This project partly utilized University of Pittsburgh Cancer Institute shared resources supported by award P30CA047904. G.K. is supported by the Ligue contre le Cancer Comité de Charente-Maritime (équipe labélisée); Agence Nationale de la Recherche (ANR) – Projets blancs; ANR under the frame of E-Rare-2, the ERA-Net for Research on Rare Diseases; Association pour la recherche sur le cancer (ARC); Cancéropôle Île-de-France; Chancellerie des universités de Paris (Legs Poix), Fondation pour la Recherche Médicale (FRM); the European Commission; the European Research Council (ERC); Fondation Carrefour; Institut National du Cancer (INCa); Inserm (HTE); Institut Universitaire de France; LeDucq Foundation; the LabEx Immuno-Oncology; the RHU Torino Lumière, the Searave Foundation; the SIRIC Stratified Oncology Cell DNA Repair and Tumor Immune Elimination (SOCRATE); the SIRIC Cancer Research and Personalized Medicine (CARPEM); and the Paris Alliance of Cancer Research Institutes (PACRI).

AUTHOR CONTRIBUTIONS

D.T. and J.J. designed the experiments. R.K., S.Z., Y.X., L.Z., J.L., Q.W., L.C., M.X., and D.T. conducted the experiments. D.T. wrote the paper. Q.R., H.W., and T.R.B. provided important reagents and samples. G.K., H.W., and T.R.B. edited and commented on the manuscript.

DECLARATION OF INTERESTS

The authors declare no conflicts of interest or financial interests.

Received: February 12, 2018

Revised: April 25, 2018

Accepted: May 18, 2018

Published: June 21, 2018

REFERENCES

Aachoui, Y., Leaf, I.A., Hagar, J.A., Fontana, M.F., Campos, C.G., Zak, D.E., Tan, M.H., Cotter, P.A., Vance, R.E., Aderem, A., et al. (2013). Caspase-11 protects against bacteria that escape the vacuole. *Science* 339, 975–978.

Aglietti, R.A., Estevez, A., Gupta, A., Ramirez, M.G., Liu, P.S., Kayagaki, N., Ciferri, C., Dixit, V.M., and Dueber, E.C. (2016). GsdmD p30 elicited by caspase-11 during pyroptosis forms pores in membranes. *Proc. Natl. Acad. Sci. USA* 113, 7858–7863.

Andujar, I., Rios, J.L., Giner, R.M., Miguel Cerda, J., and Recio Mdel, C. (2012). Beneficial effect of shikonin on experimental colitis induced by dextran sulfate sodium in BALB/c mice. *Evid. Based Complement. Alternat. Med.* 2012, 271606.

Boyum, A. (1968). Isolation of mononuclear cells and granulocytes from human blood. Isolation of monuclear cells by one centrifugation, and of granulocytes by combining centrifugation and sedimentation at 1 g. *Scand. J. Clin. Lab. Invest. Suppl.* 97, 77–89.

Brigelius-Flohe, R., and Maiorino, M. (2013). Glutathione peroxidases. *Biochim. Biophys. Acta* 1830, 3289–3303.

Brutsch, S.H., Rademacher, M., Roth, S.R., Muller, K., Eder, S., Viertel, D., Franz, C., Kuhn, H., and Borchert, A. (2016). Male subfertility induced by heterozygous expression of catalytically inactive glutathione peroxidase 4 is rescued in vivo by systemic inactivation of the Alox15 gene. *J. Biol. Chem.* 291, 23578–23588.

Canli, O., Alankus, Y.B., Grootjans, S., Vegi, N., Hultner, L., Hoppe, P.S., Schroeder, T., Vandenabeele, P., Bornkamm, G.W., and Greten, F.R. (2016). Glutathione peroxidase 4 prevents necroptosis in mouse erythroid precursors. *Blood* 127, 139–148.

Chen, L., Hambright, W.S., Na, R., and Ran, Q. (2015). Ablation of the ferroptosis inhibitor glutathione peroxidase 4 in neurons results in rapid motor neuron degeneration and paralysis. *J. Biol. Chem.* 290, 28097–28106.

Cheng, K.T., Xiong, S., Ye, Z., Hong, Z., Di, A., Tsang, K.M., Gao, X., An, S., Mittal, M., Vogel, S.M., et al. (2017). Caspase-11-mediated endothelial pyroptosis underlies endotoxemia-induced lung injury. *J. Clin. Invest.* 127, 4124–4135.

Ding, J., Wang, K., Liu, W., She, Y., Sun, Q., Shi, J., Sun, H., Wang, D.C., and Shao, F. (2016). Pore-forming activity and structural autoinhibition of the gasdermin family. *Nature* 535, 111–116.

Friedmann Angeli, J.P., Schneider, M., Proneth, B., Tyurina, Y.Y., Tyurin, V.A., Hammond, V.J., Herbach, N., Aichler, M., Walch, A., Eggenhofer, E., et al. (2014). Inactivation of the ferroptosis regulator Gpx4 triggers acute renal failure in mice. *Nat. Cell Biol.* 16, 1180–1191.

Gaschler, M.M., and Stockwell, B.R. (2017). Lipid peroxidation in cell death. *Biochem. Biophys. Res. Commun.* 482, 419–425.

Guo, Z., Ran, Q., Roberts, L.J., 2nd, Zhou, L., Richardson, A., Sharan, C., Wu, D., and Yang, H. (2008). Suppression of atherosclerosis by overexpression of glutathione peroxidase-4 in apolipoprotein E-deficient mice. *Free Radic. Biol. Med.* 44, 343–352.

Hagar, J.A., Powell, D.A., Aachoui, Y., Ernst, R.K., and Miao, E.A. (2013). Cytoplasmic LPS activates caspase-11: implications in TLR4-independent endotoxic shock. *Science* 341, 1250–1253.

Hayashi, T., Mo, J.H., Gong, X., Rossetto, C., Jang, A., Beck, L., Elliott, G.I., Kufareva, I., Abagyan, R., Broide, D.H., et al. (2007). 3-Hydroxyanthranilic acid inhibits PDK1 activation and suppresses experimental asthma by inducing T cell apoptosis. *Proc. Natl. Acad. Sci. USA* 104, 18619–18624.

He, W.T., Wan, H., Hu, L., Chen, P., Wang, X., Huang, Z., Yang, Z.H., Zhong, C.Q., and Han, J. (2015). Gasdermin D is an executor of pyroptosis and required for interleukin-1 β secretion. *Cell Res.* 25, 1285–1298.

Imai, H., and Nakagawa, Y. (2003). Biological significance of phospholipid hydroperoxide glutathione peroxidase (PHGPx, GPx4) in mammalian cells. *Free Radic. Biol. Med.* 34, 145–169.

Jorgensen, I., Rayamajhi, M., and Miao, E.A. (2017). Programmed cell death as a defence against infection. *Nat. Rev. Immunol.* 17, 151–164.

Jorgensen, I., Zhang, Y., Krantz, B.A., and Miao, E.A. (2016). Pyroptosis triggers pore-induced intracellular traps (PITs) that capture bacteria and lead to their clearance by efferocytosis. *J. Exp. Med.* 213, 2113–2128.

Kadamur, G., and Ross, E.M. (2013). Mammalian phospholipase C. *Annu. Rev. Physiol.* 75, 127–154.

Kagan, V.E., Mao, G., Qu, F., Angeli, J.P., Doll, S., Croix, C.S., Dar, H.H., Liu, B., Tyurin, V.A., Ritov, V.B., et al. (2017). Oxidized arachidonic and adrenic PEs navigate cells to ferroptosis. *Nat. Chem. Biol.* 13, 81–90.

Kayagaki, N., Stowe, I.B., Lee, B.L., O'Rourke, K., Anderson, K., Warming, S., Cuellar, T., Haley, B., Roose-Girma, M., Phung, Q.T., et al. (2015). Caspase-11 cleaves gasdermin D for non-canonical inflammasome signalling. *Nature* 526, 666–671.

Kayagaki, N., Warming, S., Lamkanfi, M., Vande Walle, L., Louie, S., Dong, J., Newton, K., Qu, Y., Liu, J., Heldens, S., et al. (2011). Non-canonical inflammasome activation targets caspase-11. *Nature* 479, 117–121.

Kayagaki, N., Wong, M.T., Stowe, I.B., Ramani, S.R., Gonzalez, L.C., Akashi-Takamura, S., Miyake, K., Zhang, J., Lee, W.P., Muszynski, A., et al. (2013). Noncanonical inflammasome activation by intracellular LPS independent of TLR4. *Science* 341, 1246–1249.

- Liu, X., Zhang, Z., Ruan, J., Pan, Y., Magupalli, V.G., Wu, H., and Lieberman, J. (2016). Inflammasome-activated gasdermin D causes pyroptosis by forming membrane pores. *Nature* 535, 153–158.
- Man, S.M., and Kanneganti, T.D. (2016). Converging roles of caspases in inflammasome activation, cell death and innate immunity. *Nat. Rev. Immunol.* 16, 7–21.
- Mannes, A.M., Seiler, A., Bosello, V., Maiorino, M., and Conrad, M. (2011). Cysteine mutant of mammalian GPx4 rescues cell death induced by disruption of the wild-type selenoenzyme. *FASEB J.* 25, 2135–2144.
- Marim, F.M., Silveira, T.N., Lima, D.S., Jr., and Zamboni, D.S. (2010). A method for generation of bone marrow-derived macrophages from cryopreserved mouse bone marrow cells. *PLoS One* 5, e15263.
- Matsushita, M., Freigang, S., Schneider, C., Conrad, M., Bornkamm, G.W., and Kopf, M. (2015). T cell lipid peroxidation induces ferroptosis and prevents immunity to infection. *J. Exp. Med.* 212, 555–568.
- Pocock, T.M., and Bates, D.O. (2001). In vivo mechanisms of vascular endothelial growth factor-mediated increased hydraulic conductivity of Rana capillaries. *J. Physiol.* 534, 479–488.
- Py, B.F., Jin, M., Desai, B.N., Penumaka, A., Zhu, H., Kober, M., Dietrich, A., Lipinski, M.M., Henry, T., Clapham, D.E., et al. (2014). Caspase-11 controls interleukin-1 β release through degradation of TRPC1. *Cell Rep.* 6, 1122–1128.
- Ran, Q., Van Remmen, H., Gu, M., Qi, W., Roberts, L.J., 2nd, Prolla, T., and Richardson, A. (2003). Embryonic fibroblasts from Gpx4 $^{-/-}$ mice: a novel model for studying the role of membrane peroxidation in biological processes. *Free Radic. Biol. Med.* 35, 1101–1109.
- Rathinam, V.A., Vanaja, S.K., Waggoner, L., Sokolovska, A., Becker, C., Stuart, L.M., Leong, J.M., and Fitzgerald, K.A. (2012). TRIF licenses caspase-11-dependent NLRP3 inflammasome activation by gram-negative bacteria. *Cell* 150, 606–619.
- Reuter, S., Gupta, S.C., Chaturvedi, M.M., and Aggarwal, B.B. (2010). Oxidative stress, inflammation, and cancer: how are they linked? *Free Radic. Biol. Med.* 49, 1603–1616.
- Ryter, S.W., Kim, H.P., Hoetzel, A., Park, J.W., Nakahira, K., Wang, X., and Choi, A.M. (2007). Mechanisms of cell death in oxidative stress. *Antioxid. Redox Signal.* 9, 49–89.
- Sborgi, L., Ruhl, S., Mulvihill, E., Pipercevic, J., Heilig, R., Stahlberg, H., Farady, C.J., Muller, D.J., Broz, P., and Hiller, S. (2016). GSDMD membrane pore formation constitutes the mechanism of pyroptotic cell death. *Embo J.* 35, 1766–1778.
- Seiler, A., Schneider, M., Forster, H., Roth, S., Wirth, E.K., Culmsee, C., Plesnila, N., Kremmer, E., Radmark, O., Wurst, W., et al. (2008). Glutathione peroxidase 4 senses and translates oxidative stress into 12/15-lipoxygenase dependent- and AIF-mediated cell death. *Cell Metab.* 8, 237–248.
- Shi, J., Zhao, Y., Wang, K., Shi, X., Wang, Y., Huang, H., Zhuang, Y., Cai, T., Wang, F., and Shao, F. (2015). Cleavage of GSDMD by inflammatory caspases determines pyroptotic cell death. *Nature* 526, 660–665.
- Shi, J., Zhao, Y., Wang, Y., Gao, W., Ding, J., Li, P., Hu, L., and Shao, F. (2014). Inflammatory caspases are innate immune receptors for intracellular LPS. *Nature* 514, 187–192.
- Singer, M., Deutschman, C.S., Seymour, C.W., Shankar-Hari, M., Annane, D., Bauer, M., Bellomo, R., Bernard, G.R., Chiche, J.D., Cooper-Smith, C.M., et al. (2016). The Third International Consensus Definitions for sepsis and septic shock (Sepsis-3). *JAMA* 315, 801–810.
- Song, X., Zhu, S., Xie, Y., Liu, J., Sun, L., Zeng, D., Wang, P., Ma, X., Kroemer, G., Bartlett, D.L., et al. (2018). JTC801 induces pH-dependent death specifically in cancer cells and slows growth of tumors in mice. *Gastroenterology* 154, 1480–1493.
- Sun, X., Ou, Z., Chen, R., Niu, X., Chen, D., Kang, R., and Tang, D. (2016). Activation of the p62-Keap1-NRF2 pathway protects against ferroptosis in hepatocellular carcinoma cells. *Hepatology* 63, 173–184.
- Tang, D., Kang, R., Livesey, K.M., Cheh, C.W., Farkas, A., Loughran, P., Hoppe, G., Bianchi, M.E., Tracey, K.J., Zeh, H.J., 3rd, et al. (2010). Endogenous HMGB1 regulates autophagy. *J. Cell Biol.* 190, 881–892.
- van Meer, G., Voelker, D.R., and Feigenson, G.W. (2008). Membrane lipids: where they are and how they behave. *Nat. Rev. Mol. Cell Biol.* 9, 112–124.
- Vanden Berghe, T., Demon, D., Bogaert, P., Vandendriessche, B., Goethals, A., Depuydt, B., Vuylsteke, M., Roelandt, R., Van Wonterghem, E., Vandebroecke, J., et al. (2014). Simultaneous targeting of IL-1 and IL-18 is required for protection against inflammatory and septic shock. *Am. J. Respir. Crit. Care Med.* 189, 282–291.
- Wilmore, J.R., Gaudette, B.T., Gomez Atria, D., Hashemi, T., Jones, D.D., Gardner, C.A., Cole, S.D., Mistic, A.M., Beiting, D.P., and Allman, D. (2018). Commensal microbes induce serum IgA responses that protect against polymicrobial sepsis. *Cell Host Microbe* 23, 302–311.e3.
- Wortmann, M., Schneider, M., Pircher, J., Hellfritsch, J., Aichler, M., Vegi, N., Kolle, P., Kuhlencordt, P., Walch, A., Pohl, U., et al. (2013). Combined deficiency in glutathione peroxidase 4 and vitamin E causes multiorgan thrombus formation and early death in mice. *Circ. Res.* 113, 408–417.
- Xie, M., Yu, Y., Kang, R., Zhu, S., Yang, L., Zeng, L., Sun, X., Yang, M., Billiar, T.R., Wang, H., et al. (2016). PKM2-dependent glycolysis promotes NLRP3 and AIM2 inflammasome activation. *Nat. Commun.* 7, 13280.
- Xie, Y., Zhu, S., Song, X., Sun, X., Fan, Y., Liu, J., Zhong, M., Yuan, H., Zhang, L., Billiar, T.R., et al. (2017a). The tumor suppressor p53 limits ferroptosis by blocking DPP4 activity. *Cell Rep.* 20, 1692–1704.
- Xie, Y., Zhu, S., Zhong, M., Yang, M., Sun, X., Liu, J., Kroemer, G., Lotze, M., Zeh, H.J., 3rd, Kang, R., et al. (2017b). Inhibition of aurora kinase induces necroptosis in pancreatic carcinoma. *Gastroenterology* 153, 1429–1443.e5.
- Yang, L., Xie, M., Yang, M., Yu, Y., Zhu, S., Hou, W., Kang, R., Lotze, M.T., Billiar, T.R., Wang, H., et al. (2014a). PKM2 regulates the Warburg effect and promotes HMGB1 release in sepsis. *Nat. Commun.* 5, 4436.
- Yang, W.S., SriRamaratnam, R., Welsch, M.E., Shimada, K., Skouta, R., Viswanathan, V.S., Cheah, J.H., Clemons, P.A., Shamji, A.F., Clish, C.B., et al. (2014b). Regulation of ferroptotic cancer cell death by GPX4. *Cell* 156, 317–331.
- Yoo, S.E., Chen, L., Na, R., Liu, Y., Rios, C., Van Remmen, H., Richardson, A., and Ran, Q. (2012). Gpx4 ablation in adult mice results in a lethal phenotype accompanied by neuronal loss in brain. *Free Radic. Biol. Med.* 52, 1820–1827.
- Yuan, H., Li, X., Zhang, X., Kang, R., and Tang, D. (2016). Identification of ACSL4 as a biomarker and contributor of ferroptosis. *Biochem. Biophys. Res. Commun.* 478, 1338–1343.
- Zeng, L., Kang, R., Zhu, S., Wang, X., Cao, L., Wang, H., Billiar, T.R., Jiang, J., and Tang, D. (2017). ALK is a therapeutic target for lethal sepsis. *Sci. Transl. Med.* 9, <https://doi.org/10.1126/scitranslmed.aan5689>.
- Zhu, S., Zhang, Q., Sun, X., Zeh, H.J., 3rd, Lotze, M.T., Kang, R., and Tang, D. (2017). HSPA5 regulates ferroptotic cell death in cancer cells. *Cancer Res.* 77, 2064–2077.

STAR★METHODS

KEY RESOURCES TABLE

REAGENT or RESOURCE	SOURCE	IDENTIFIER
Antibodies		
Rabbit monoclonal [EPNCIR144] to GPX4	Abcam	ab125066; RRID:AB_10973901
Rabbit polyclonal to caspase-1	Abcam	ab1872; RRID:AB_302644
Goat polyclonal to IL-1 β	R&D Systems	AF-401-NA; RRID:AB_416684
Rabbit polyclonal to GSDMD	Sigma-Aldrich	G7422; RRID:AB_1850381
Mouse monoclonal to caspase-1	AdipoGen	AG-20B-0042; RRID:AB_2490248
Mouse monoclonal [A-7] to GSDMD	Santa Cruz Biotechnology	Sc-393656; RRID: AB_2728694
Mouse monoclonal [64-Y] to GSDMD	Santa Cruz Biotechnology	Sc-81868; RRID: AB_2263768
Rabbit polyclonal to PLCG1	Cell Signaling Technology	2822; RRID:AB_10691689
Rabbit monoclonal [D6M9S] to phospho-PLCG1 (Tyr783)	Cell Signaling Technology	14008; RRID: AB_2728690
Rabbit monoclonal [D9D6S] to PLCB3	Cell Signaling Technology	14247; RRID: AB_2728691
Rabbit monoclonal [D8K2R] to phospho-PLCB3 (Ser537)	Cell Signaling Technology	29021; RRID: AB_2728692
Mouse monoclonal [8H10D10] to actin	Cell Signaling Technology	3700; RRID:AB_2242334
Rat monoclonal [17D9] to caspase-11	Cell Signaling Technology	14340; RRID: AB_2728693
Rabbit polyclonal to HMGB1	Cell Signaling Technology	2822; RRID:AB_10691689
Chemicals, Peptides, and Recombinant Proteins		
<i>Escherichia coli</i> LPS 0111:B4	Sigma-Aldrich	L4391
Vitamin E	Sigma-Aldrich	258024
Necrostatin-1	Sigma-Aldrich	N9037
Z-VAD-FMK	Sigma-Aldrich	V116
Wedelolactone	Sigma-Aldrich	W4016
PA	Sigma-Aldrich	P9511
DAG	Sigma-Aldrich	D8394
Linoleic acid	Sigma-Aldrich	L1376
Ceramide	Sigma-Aldrich	22244
Cholesterol	Sigma-Aldrich	C8667
U73122	Sigma-Aldrich	662035
Gentamicin	Sigma-Aldrich	G1397
Ferostatin-1	Selleck Chemicals	S7243
ATP	InvivoGen	tIrl-atp
Poly(I:C)	InvivoGen	31852-29-6
Pam3CSK4	InvivoGen	tIrl-pms
PI4P	Echelon Biosciences Incorporated	P-4004
PI(4,5)P2	Echelon Biosciences Incorporated	P-4508
BAPTA-AM	Calbiochem	126150-97-8
Lipofectamine 3000	Invitrogen	L3000-015
Puromycin	InvivoGen	ant-pr-1
SuperSignal West Pico Chemiluminescent Substrate	Thermo Fisher Scientific	34080
SuperSignal West Femto Maximum Sensitivity Substrate	Thermo Fisher Scientific	34095
Critical Commercial Assays		
Cell Counting Kit-8 (CCK-8)	Dojindo Laboratories	CK04
HMGB1 ELISA Kit	Shino Test Corporation	ST51011
IL-1 β ELISA Kit	R&D Systems	MLB00C
IL-18 ELISA Kit	R&D Systems	7625
IL-12 ELISA Kit	R&D Systems	DY419

(Continued on next page)

Continued

REAGENT or RESOURCE	SOURCE	IDENTIFIER
IL-17 ELISA Kit	R&D Systems	DY421
LDH Assay Kit	Abcam	ab102526
MDA Assay Kit	Abcam	ab118970
4-HNE Assay Kit	MyBioSource	MBS702101
DAG Assay Kit	Cell Biolabs	MET-5028
IP3 Assay Kit	LifeSpan Biosciences	LS-F10644-1
CK single-slide test	IDEXX	98-11073-01
BUN single-slide test	IDEXX	98-11070-01
ALT single-slide test	IDEXX	98-11067-01
iScript cDNA Synthesis Kit	Bio-Rad	1708890
4%–12% Criterion XT Bis-Tris gels	Bio-Rad	3450124
PVDF membranes	Bio-Rad	1620233
Experimental Models: Cell Lines		
THP1	ATCC	TIB-202
HL-60	ATCC	CCL-240
HeLa	ATCC	CCL-2
<i>Escherichia coli</i>	ATCC	11775
Experimental Models: Organisms/Strains		
<i>Gsdmd</i> ^{J105N/J105N} mice	Kayagaki et al., 2015	N/A
<i>Casp11</i> ^{flox/flox} mice	This study	N/A
<i>Gpx4</i> ^{flox/flox} mice	Yoo et al., 2012	N/A
<i>LysM-Cre</i> mice	The Jackson Laboratory	004781
<i>Alb-Cre</i> mice	The Jackson Laboratory	003574
<i>Nalp3</i> ^{-/-} mice	The Jackson Laboratory	021302
<i>Casp1</i> ^{-/-} <i>Casp11</i> ^{-/-} mice	The Jackson Laboratory	016621
Oligonucleotides		
Mouse <i>Plcg1</i> -shRNA-1 (Sequence:CCGGGCCAGCTTGTAGCACTCAAT TCTCGAGAATTGAGTGCTACAAGCTGGCTTTTT)	Sigma-Aldrich	TRCN0000024974
Mouse <i>Plcg1</i> -shRNA-2 (Sequence:CCGGCCAACCTTTCAAGTGTGCAGTA CTCGAGTACTGCACACTTGAAGTTGGTTTTT)	Sigma-Aldrich	TRCN0000024976
Human <i>Plcg1</i> -shRNA (Sequence:GTACCGGAGAAGTTCCTTCAGTACA ATCCTCGAGGATTGACTGAAGGAAGTCTTTTTTTG)	Sigma-Aldrich	TRCN0000218478
See Table S2 for primers used for qPCR	This paper	Table S2
Software and Algorithms		
Image Lab software	Bio-Rad	1709691
GraphPad Prism 7	GraphPad Software	https://www.graphpad.com/scientific-software/prism/

CONTACT FOR REAGENT AND RESOURCE SHARING

Further information and requests for reagents may be obtained from the lead contact, Daolin Tang (Email: tangd2@upmc.edu).

EXPERIMENTAL MODEL AND SUBJECT DETAILS

Cell Culture

THP1 (#TIB-202, male), HL-60 (#CCL-240, female), and HeLa (#CCL-2, female) cell lines were obtained from American Type Culture Collection (ATCC). BMDMs from male mice were obtained using 30% L929-cell conditioned medium as a source of granulocyte/macrophage colony stimulating factor ([Marim et al., 2010](#)). Mouse PMs were isolated from male mice as previously described ([Andujar et al., 2012](#)). Primary PBMCs were isolated from whole blood of male or female using the Ficoll-Paque method ([Boyum,](#)

1968). These cells were cultured in Dulbecco's Modified Eagle's Medium (#11995073, ThermoFisher Scientific) supplemented with 10% heat-inactivated fetal bovine serum (#TMS-013-B, Millipore) and 1% penicillin and streptomycin (#15070-063, ThermoFisher Scientific) at 37°C, 95% humidity, and 5% CO₂. All cells used were authenticated using STR profiling and mycoplasma testing was negative.

Bacterial Infection

Escherichia coli (#11775) were obtained from ATCC and then added to cells at a multiplicity of infection (MOI) of 25 in media without antibiotics. After 30 min, cells were washed and incubated for 1.5 h at 37°C in fresh medium supplemented with gentamicin (100 µg/ml, #G1397, Sigma Aldrich) to kill extracellular bacteria.

Animal Model of Sepsis

We conducted all animal care and experiments in accordance with the Association for Assessment and Accreditation of Laboratory Animal Care guidelines (<http://www.aaalac.org>) and with approval from our Institutional Animal Care and Use Committee. Mice were housed with their littermates in groups of four or five animals per cage and kept on a regular 12 hr light and dark cycle in a specific pathogen-free barrier facility.

Gsdmd^{105N/105N} mice (C57BL/6) were a gift from Dr. Vishva M. Dixit (Genentech, South San Francisco, CA, USA). *Casp11*^{fllox/fllox} mice (C57BL/6) were a gift from Dr. Timothy R. Billiar (University of Pittsburgh). *Gpx4*^{fllox/fllox} mice (C57BL/6) were a gift from Dr. Qitao Ran (University of Texas Health Science Center). *LysM-Cre* (#004781), *Alb-Cre* (#003574), *Nalp3*^{-/-} (#021302), and *Casp1*^{-/-}*Casp11*^{-/-} (#016621) mice were obtained from The Jackson Laboratory. These mice were used to generate indicated transgenic mice as described in the text.

Sepsis was induced in male or female C57BL/6 mice (eight- to 10-weeks old, 22 to 26 g body weight) using a surgical procedure termed cecal ligation and puncture (CLP) as previously described (Xie et al., 2016; Yang et al., 2014a). Briefly, anesthesia was induced with ketamine (80-100 mg/kg/i.p., #1867-66-9, Cayman Chemical) and xylazine (10-12.5 mg/kg/i.p., #S2516, Selleck Chemicals). A small midline abdominal incision was made and the cecum was exteriorized and ligated with 4-0 silk immediately distal to the ileocecal valve without causing intestinal obstruction. The cecum was then punctured twice with a 17-27-gauge needle. The abdomen was closed in two layers and mice were injected subcutaneously with 1 mL Ringer's solution.

Blood was collected at indicated time points, allowed to clot for 2 hr at room temperature, and then centrifuged for 15 min at 1,500×g. Serum samples were stored at -80°C before analysis. Mortality was recorded for up to 10 days after the onset of lethal sepsis to ensure that no additional late deaths occurred.

Patient Samples

PBMCs from patients with sepsis (n=16) at hospital admission and healthy controls (n = 16) were collected from Daping Hospital and Xiangya Hospital by a density gradient centrifugation method using Ficoll Histopaque. The subjects were not involved in previous procedures and test naïve. Clinical characteristics of sepsis patients and healthy control individuals including sex and age are shown in our previous publication (Table S1) (Zeng et al., 2017). Collection of samples was approved by the Institutional Review Board. Sepsis was identified according to The Third International Consensus Definitions for Sepsis and Septic Shock (Sepsis-3) (Singer et al., 2016). No statistical methods were used to pre-determine sample sizes. We did not analysis of the influence (or association) of sex, gender identity, or both on the results of the study because a small sample size for each subgroup.

METHOD DETAILS

Biochemical Assay

Commercially available enzyme linked immunosorbant assay (ELISA) kits were used to measure the concentrations of HMGB1 (#ST51011, Shino Test Corporation), IL-1β (#MLB00C, R&D Systems), IL-18 (#7625, R&D Systems), IL-12 (#DY419, R&D Systems), IL-17 (#DY421, R&D Systems), LDH (#ab102526, Abcam), MDA (#ab118970, Abcam), 4-HNE (#MBS702101, MyBioSource), DAG (#MET-5028, Cell Biolabs), and IP3 (LS-F10644-1, LifeSpan Biosciences) in serum, culture medium, or whole cell lysate according to the manufacturer's instructions. Measurement of serum tissue enzymes (CK, BUN, and ALT) were performed using the IDEXX Catalyst Dx Chemistry Analyzer according to the manufacturer's protocol.

Calcium Measurement

The intracellular Ca²⁺ concentration was detected using the fluorescent probe Fura-2 (#F1201) from Thermo Fisher Scientific according to the manufacturer's protocol. Briefly, intracellular calcium concentrations were calculated from the ratio of background corrected Fura-2 emission (520 nm) at two excitation wavelengths (340 nm/380 nm) using a microplate reader (Cytation 5 Cell Imaging Multi-Mode Reader, BioTek, USA).

LPS Transfection

To stimulate caspase-11 noncanonical inflammasome activation, LPS were electroporated into indicated cells using the Neon Transfection System (Thermo Fisher Scientific) according to the manufacturer's protocol. Briefly, 1 × 10⁶ BMDMs were electroporated LPS (1-3 µg) in buffer R (#MPK10025, Thermo Fisher Scientific) under pulse voltage 1400V, pulse width 10ms, and pulse number 2.

RNAi and Gene Transfection

Mouse PLCG1-shRNA (#TRCN0000024974 and #TRCN0000024976), human PLCG1-shRNA (#TRCN0000218478), and control-shRNA (#SHC001) were obtained from Sigma (St. Louis, MO, USA). GSDMD-N (1-276), GSDMD-C (277-487), GSDMD cleavage mutant (D275A), and full-length WT GSDMD plasmids were a kind gift from Dr. Feng Shao (National Institute of Biological Sciences in China) (Ding et al., 2016). The Gpx4 cDNA expression construct was a gift from Dr. Qitao Ran (University of Texas Health Science Center). Inactive Gpx4 cDNA (U46S mutant) was generated as previously described (Mannes et al., 2011). Transfection was performed using lentiviral vector or Lipofectamine 3000 (#L3000-015, Invitrogen, Grand Island, NY, USA,) according to the manufacturer's instructions (Xie et al., 2017b). Puromycin (#ant-pr-1; InvivoGen) was used to generate stable knockdown cell lines.

Western Blot Analysis

Western blot was used to analyze protein expression as described previously (Sun et al., 2016; Tang et al., 2010; Xie et al., 2017a). In brief, after extraction, proteins in cell lysates were first resolved by 4%–12% Criterion XT Bis-Tris gel electrophoresis and then transferred to polyvinylidene difluoride membrane and subsequently incubated with the primary antibody (1:500-1:1000). After incubation with peroxidase-conjugated secondary antibodies (1:1000-1:2000), the signals were visualized by enhanced chemiluminescence (#32106, Thermo Fisher Scientific) according to the manufacturer's instructions.

Quantitative Real-Time Polymerase Chain Reaction

Total RNA was extracted using TRI reagent (#93289, Sigma Aldrich) according to the manufacturer's instructions. First-strand cDNA was synthesized from 1 μ g of RNA using the iScript cDNA Synthesis kit (#1708890, Bio-Rad). cDNA from various cell samples was amplified using real-time quantitative PCR with specific primers (Table S2). The data were normalized to 18S RNA and the fold change was calculated via the $2^{-\Delta\Delta C_t}$ method (Song et al., 2018; Zhu et al., 2017). Relative concentrations of mRNA were expressed in arbitrary units based on the untreated group, which was assigned a value of 1.

QUANTIFICATION AND STATISTICAL ANALYSIS

Statistical Analysis

Data are presented as mean \pm SD. All data meet the assumptions of the tests (e.g., normal distribution). Unpaired Student's t tests were used to compare the means of two groups. One-way Analysis of Variance (ANOVA) was used for comparison among the different groups. When ANOVA was significant, *post hoc* testing of differences between groups was performed using the Least Significant Difference (LSD) test. The Kaplan-Meier method was used to compare differences in mortality rates between groups. A p value < 0.05 was considered statistically significant. The exact value of n within figures was indicated in figure legends. We did not exclude samples or animals. For every figure, statistical tests are justified as appropriate. All data meet the assumptions of the tests. No statistical methods were used to pre-determine sample sizes, but our sample sizes are similar to those generally employed in the field.